Impingement Studies For G-DI Spays At Elevated Temperatures

Kay P.J., Morris D.W., Bowen P.J., Gold M.R.* and Sapsford S.M.*
Mechanical Engineering Division, Cardiff University, School of Engineering, Queens Buildings, PO Box 925, Cardiff, CF24 OYF, UK.
*Ricardo Consulting Engineers, Bridge Works, Shoreham-by-Sea, Sussex, UK.

Abstract

This paper describes a new facility that allows optical-based, temporally-resolved spray impingement studies under conditions of elevated temperature (independent control of air and surface) and ambient pressure, allowing variation of the injector-piston orientation. The data presented and analysed in this paper has been obtained utilising temporally-resolved Phase Doppler Anemometry, and high-speed imaging of the spray and the residual fuel film. The paper analyses the characteristics of the secondary spray relative to the primary, as well as the evaporation timescale for the residual fuel film. Results are discussed in light of contemporary model predictions for this type of scenario, and related to the application of Gasoline Direct Injection (G-DI).

1. Introduction

Impingement is inevitable in G-DI engines given the spray penetration rate of current G-DI injectors and the dimensions of the combustion chamber of typical automotive engines. The impingement process is a very important part of the mixture preparation process, and must be understood in greater detail to optimise the fuel transportation, minimise pollutant formation - particularly unburnt hydrocarbons and particulate matter - and develop new, validated, models.

Impingement is a process with broader application than the G-DI engine (e.g. spray paint coating, spray cooling systems, etc). Several recent, informative reviews have been published, and these provide useful benchmarks for the current investigation. The study of Özdemir & Whitelaw [1] is notable in that it provides a basis for laser diagnostic investigations of impinging sprays and proposes a method for differentiating between primary and secondary spray from experimental data. They also provide a phenomenological proposal for the flow field structure of a typical impinging spray. Bai et al [2] suggest a current method for modelling impinging sprays, suitable for inclusion in more general CFD models. Finally Tropea & Roisman [3] provide an insight into future challenges for modelling the complexities of the spray impingement process, emphasising the stochastic nature of the process, and the need for modelling approaches to accommodate this feature.

Previous studies by Cardiff and Ricardo have concentrated on the development of ‘tools and techniques’ for investigating and appraising two-phase aspects of ‘free’ sprays. These have included optimising methods for undertaking appropriate temporally-resolved measurements for a wide variety of injectors, injector operating conditions and ambient environment. Here, the aim is to extend this capability to facilitate systematic, fundamental investigations of impinging sprays with independent control of the relevant variables and dimensionless groups, again providing temporally-resolved data-sets for CFD model appraisal or the development of new empirical sub-models for the impingement process. Data is analysed and appraised in terms of its sensibility, and compared against conclusions from the aforementioned studies and model predictions.

2. Experimental Techniques and Facility Development

All the techniques used to study the spray outlined in this paper were performed in the Cardiff/Ricardo High Temperature-High Pressure (HT-HP) test rig shown in Figure 1. The test rig is discussed in more detail by Comer et al. [4] and currently facilitates spray characterisation under controlled conditions up to 30 bar and 673K. The HT-HP rig has been modified such that a flat piston, which can be heated and accurately controlled up to 483K, can be positioned within the HT-HP environment, allowing optical diagnostic studies of the impingement process under hot and cold surface conditions. The piston is mounted on an internal 'jig', to readily facilitate accurately 3D positioning relative to the injector spray axis.

The piston-temperature controller allows heating to temperatures within the range 475-573K, pertinent to conditions in fired engines [5]. Hence the HT-HP rig allows primary variables relevant to the G-DI application to be systematically studied under controlled conditions.

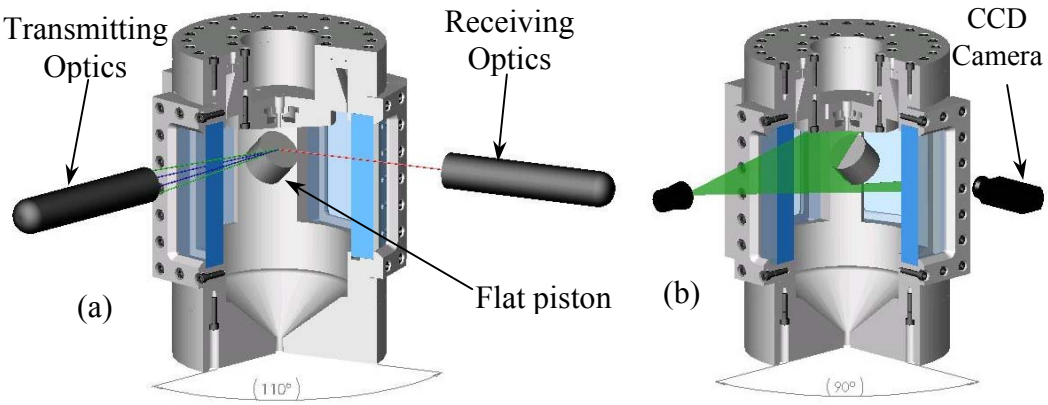

Figure 1: Model of the HT-HP rig setup for (a) PDA and (b) planar imaging diagnostics.

The same 70° pressure-swirl injector was used throughout the programme for both the free and impinging studies and the fuel used was regular unleaded gasoline, injected at a line pressure of 100 bar with an injection duration of 1.5 ms. The same conditions were maintained throughout all the experiments, namely atmospheric air pressure, P_a = 0.1 MPa, atmospheric air temperature, T_a, and a raised piston temperature for the impingement case, T_p, of 423K. The piston itself is constructed from aluminium, with a surface polished to a roughness, r, of 0.39 μm, hence $D_{32} >> r$. It is angled at 45 degrees to the spray axis, and coincides with the central axis 35mm downstream.

Figure 2 shows the points where the control volume for the phase Doppler anemometer (PDA) were positioned within the central plane of the spray, note all the points are referenced from the centre of the injector orifice (0,0). The points for the free spray were chosen such that the first and last points show the edge of the spray. The grid positions chosen for the impinging case were chosen such that they coincide with the free spray points to allow direct comparison. Three representative points of interest have been chosen for discussion as illustrated in Figure 2. For the free spray PDA data, symmetry is assumed, and hence data only for one half of the spray was generated [6].

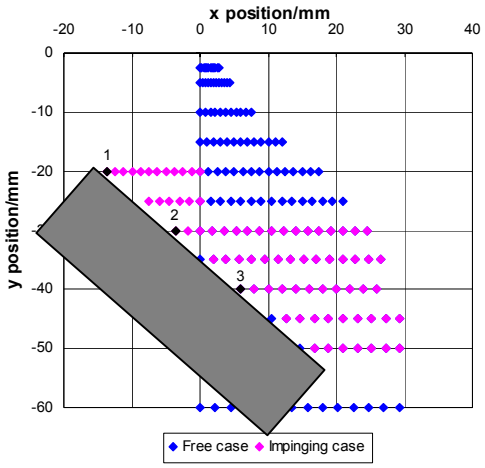

Figure 2: Schematic showing where the points for the PDA data was taken for the free and impinging case.

The optical configuration for the PDA set-up is identical to that utilised in previous studies. Of note, is that the geometrical configuration of the piston orientation and optical access still facilitates data collection from first-order scattering. The hardware/software set-up and post-processing algorithms for time-resolved data are essentially the same as those outlined previously [7], though some additional post-processing software development was required to present the impingement data in a suitable form for discussion and analysis.

Data rates and validation rates were not significantly different from those consistently recorded for optimal set-up and measurement in the free spray environment, indicating good quality of data.

3. Results

Figures 5 & 6 (a) Free & (c) Impingement show the raw PDA data, for the first 5ms, presented in two ways. Firstly as the vertical velocity component, positive velocity is taken as downwards, plotted against the horizontal velocity component, positive velocity is taken to the right. Hence any point on the 'pink' dashed line represents a droplet with equal horizontal and vertical components, i.e. the particle is travelling parallel to the surface of the piston.

Secondly, with the resolved velocity component normal to the piston surface plotted against droplet diameter. Figures 5 & 6 (b) Free & (d) Impingement show the raw resolved data bounded lines corresponding to the critical Weber numbers as suggested by Bai et al [2]. The critical Weber numbers for the regime transitions are shown in Table 1.

Table 1: Regime transition conditions [2]

Surface Condition	Regime	Critical Weber Number
Dry	Stick/Spread → Splash	$We_c \approx 2630.La^{-0.183}$
Wetted	Stick → Rebound	$We_c \approx 2$
	Rebound → Spread	$We_c \approx 20$
	Spread → Splash	$We_c \approx 1320.La^{-0.183}$

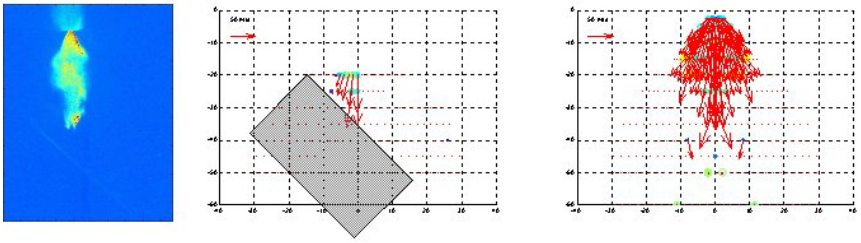

1.00ms after start of injection (SOI)

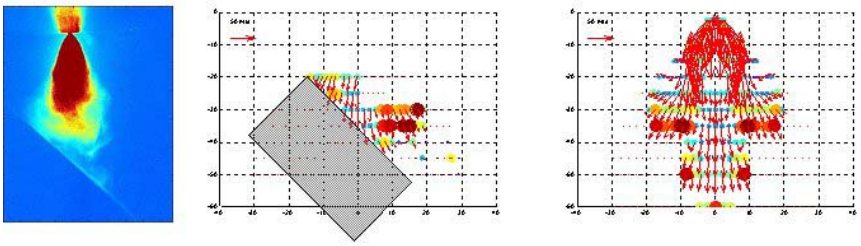

1.50ms after SOI

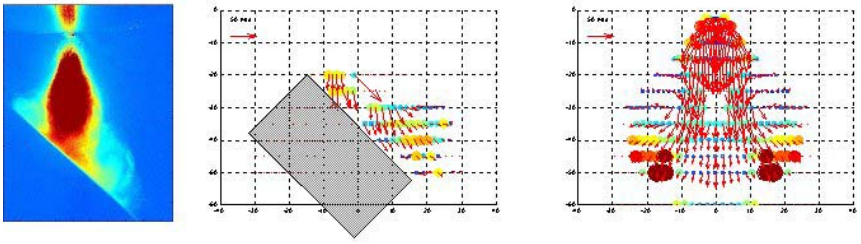

2.00ms after SOI

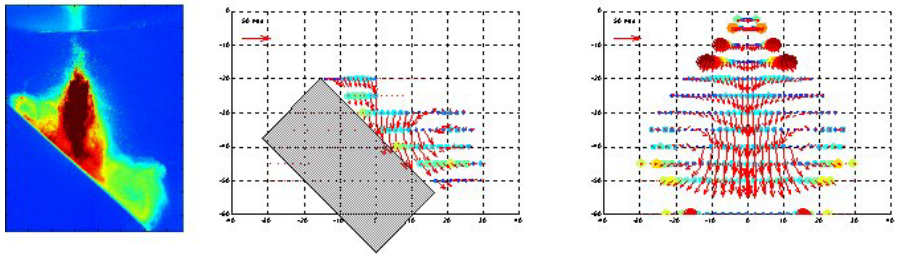

2.50ms after SOI

Figure 3: Sequence showing form left to right: Enhanced high-speed photography, processed PDA data for impinging case and free case respectively.

0.998s after impingement

1.008s after impingement

Figure 4: Enhanced high-speed photography of the fuel film evaporating.

The data for the free case has been plotted in the same way as for the impinging case, i.e. with velocities resolved normal to the piston surface, even though obviously the piston surface is not present, hence the droplets cannot have a velocity normal to the piston. This is to facilitate a direct comparison with the impinging data set.

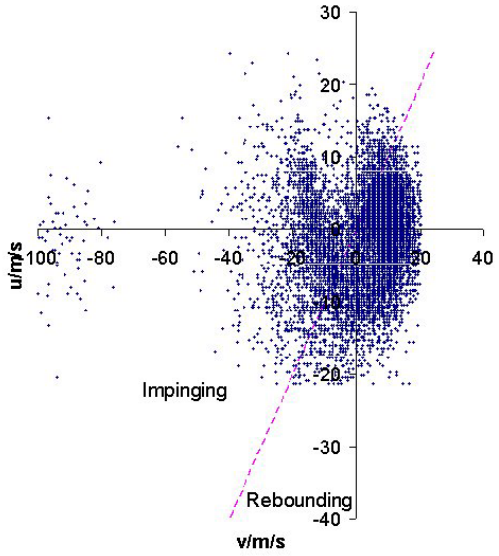

(a) Free

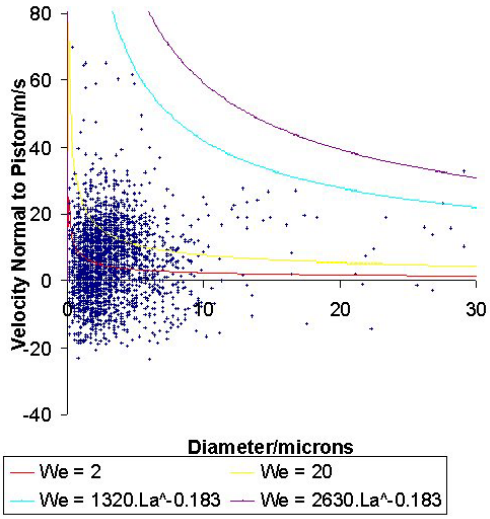

(b) Free

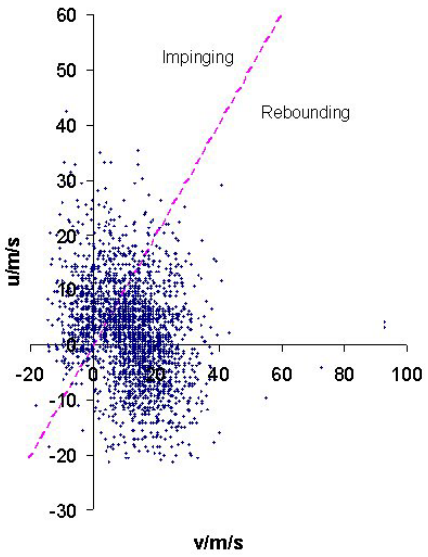

(c) Impinging

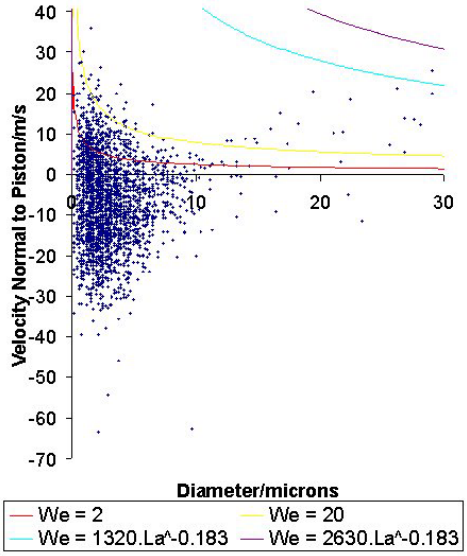

(d) Impinging

Figure 5: Processed data for point 1. (a) velocity vectors and (b) resolved velocities for the free spray, and (c) the velocity vectors and (d) resolved velocities for the impinging case.

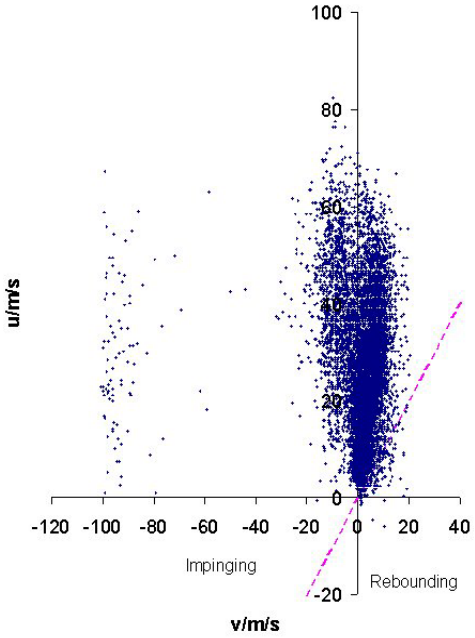

(a) Free

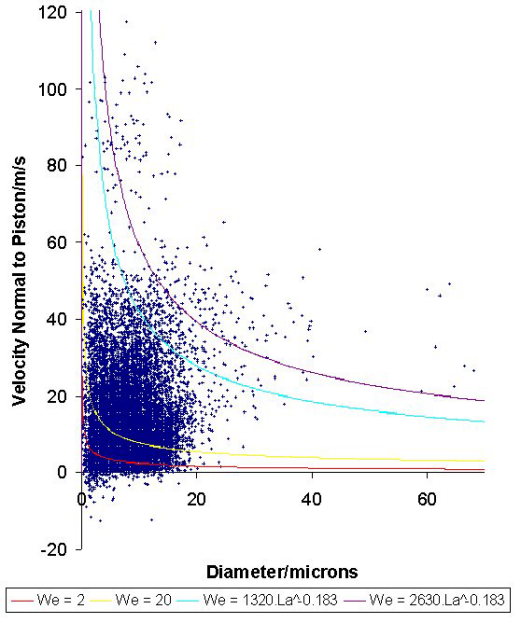

(b) Free

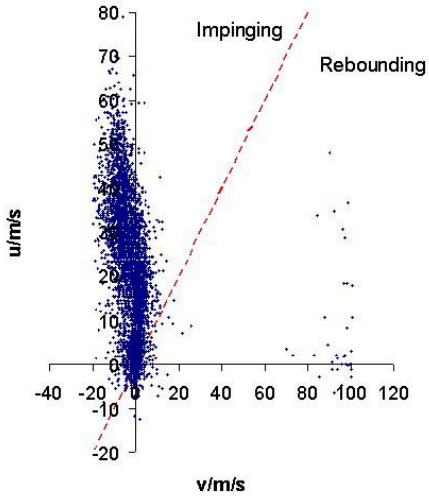

(c) Impinging

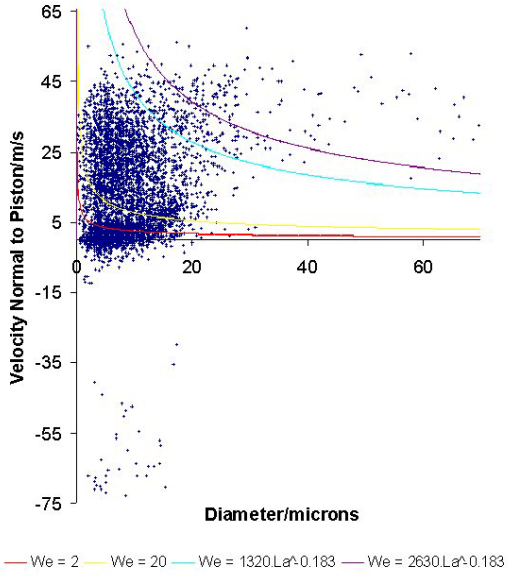

(d) Impinging

Figure 6: Processed data for the point 2. (a) velocity vectors and (b) resolved velocities for the free spray, and (c) the velocity vectors and (d) resolved velocities for the impinging case.

4. Analysis and Discussion

The vortices observed in the post processed PDA data and the enhanced high-speed digital photography (Figure 3) are consistent with a previous phenomenological interpretation. Özdemir & Whitelaw [1] studied the impingement of an axis-symmetric jet on heated and unheated flat plates, and a schematic representation of their findings is shown in Figure 7. The figure also shows vortices moving upstream and a relatively large vortex that has formed downstream, as clearly observed in Figure 3 compiled from the current dataset.

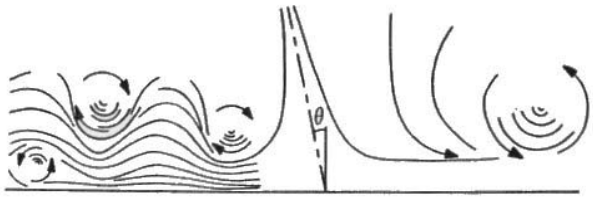

Figure 7: Schematic of the flow visualisation of a jet impinging on a flat plate by Özdemir & Whitelaw [1]

The enhanced high-speed video images in Figure 3 show the fuel film evaporating from the flat piston at the elevated temperature of 423K; the total time for the fuel film to evaporate under these conditions is 0.118 seconds, indicating that without convective heat transfer effects, impingement would occur on wetted surfaces. Furthermore, even for a single injection, once the pre-spray has initially wetted the piston surface, then the proceeding main spray will effectively be impinging on a wetted surface. Hence, it is suggested the wetted transition regimes suggested by Bai et al [2] are appropriate for comparison with this data, though correlations for un-wetted impingement are also included for comparative purposes.

In the resolved component plots (Figures 5 & 6), it is apparent that on a droplet number count basis, the majority of the droplet population (<20 μm) are not predicted to splash, i.e. they either stick, rebound or spread. However, for the remaining larger droplets (>30μm), the majority are predicted to splash due to their relatively higher Weber numbers. Clearly the characteristics required of the primary spray change according to the purpose and conditions of the impingement process, offering potential design considerations for optimisation of spray-piston interaction. Hence, converting these into a mass basis, indicates that for points 1, 2 & 3 approximately half of the primary spray mass is predicted to either splash or rebound.

Figure 6 shows the processed PDA data for point 2. Comparing plots (b) and (d), the free case shows droplets with velocities normal to the surface of the piston up to 100 m/s compared to maximum values of 65 m/s for the impinging case, showing tat the addition of the piston changes the structure of the primary spray. Another general observation is that there are a larger number of droplets for the impinging case with negative velocities normal to the piston, suggesting that these droplets have rebounded or splashed from the surface of the piston. Plot (d) shows a 'group' of droplets with a high negative velocities normal to the piston, which suggests that these droplets have rebounded rather than splashed from the piston surface as they still have velocities comparable to the primary spray, i.e. that the Weber number for each of these droplets was within the range of 2-20 [Bai et al, 2002].

The velocity components in Figure 5 show, both for the free and impinging case, that there are a large number of droplets with negative normal velocity. This can be explained for the free spray case by examining Figure 3, which shows in the sequence a vortex forming due to the fuel being sprayed into a quiescent atmosphere. However, the vortex cannot be present for the impinging case as it encounters the piston. Therefore the droplets with a negative normal velocity are droplets in the secondary spray i.e. they have impinged on the

piston surface and either rebounded, splashed or have been entrained in the downstream turbulent vortices as observed by Özdemir & Whitelaw [1].

The processed PDA data for point 3, although not presented her shows similar trends to those for point 2. At this point the effect of introducing the piston is not a evident as the other 2 points. This can be explained by considering the spatial position for this particular point. It is in a position where, due to the swirl spray characteristics, the droplets are moving radially outwards and consequently have a lower normal velocity component compared to positions closer to the injector axis, this can be verified by comparing the velocity plots. It can also be shown that the droplets in the impinging case have a slightly higher radial velocity due to the interaction between the droplets themselves and the piston surface, as shown schematically in Figure 7.

5. Conclusion

- A new facility has been commissioned that allows non-intrusive optical measurements for temporally-resolved size and velocity components of sprays under controlled conditions representative of G-DI operation. Good quality PDA data was achieved, facilitating temporally-resolved data after appropriate post-processing.
- This first impingement data-set in the new facility shows consistency with a previous 'free' spray characterisation for the same injector, as well as phenomenological interpretations of the spray flowfield post-impingement by other investigators.
- Two methods of post-processing the data to differentiate between primary and secondary spray have been considered, and both have proven useful and informative in identifying impingement trends. The secondary spray can be clearly identified when comparing data for the 'impinging' spray with the corresponding 'free' spray.
- A comparison of the current data-set with a model proposed in the literature, indicates that under conditions considered in this study, approximately half of the primary spray mass contributes to a secondary spray (rebound/splash). This needs further verification, and to be taken into consideration for the G-DI application.

References

[1] Özdemir I.B & Whitelaw J.H., *J. Fluid Mech.* V240, pp 503-532, 1991.
[2] Bai C.X., Rusche H., and Gosman A.D, *Atomization and Sprays*, V12, pp 1-27, 2002.
[3] Tropea C & Roisman IV, *Atomisation and Sprays*, V10, pp. 387-408, 2000.
[4] Comer MA, Bowen PJ, Sapsford SM, Bates CJ and John RJR, *Atomisation and Sprays*, V9 (5), pp. 467-482, Nov. 1999.
[5] Karlson RB & Heywood JB, SAE paper 2001-01-2022, 2001.
[6] Comer MA, Ph.D Thesis, University of Wales, Cardiff, 1999.
[7] Comer M.A., Morris D.W., Bowen PJ, Sapsford SM and Bates CJ,*17th Annual ILASS-EUROPE*, Zurich 2001.